

Space-time crystals of trapped ions

Tongcang Li,¹ Zhe-Xuan Gong,^{2,3} Zhang-Qi Yin,^{3,4} H. T. Quan,⁵
Xiaobo Yin,¹ Peng Zhang,¹ L.-M. Duan,^{2,3} and Xiang Zhang^{1,6,*}

¹*NSF Nanoscale Science and Engineering Center, 3112 Etcheverry Hall,
University of California, Berkeley, California 94720, USA*

²*Department of Physics, University of Michigan, Ann Arbor, Michigan 48109, USA*

³*Center for Quantum Information, Institute of Interdisciplinary Information Science,
Tsinghua University, Beijing, 100084, P. R. China*

⁴*Key Laboratory of Quantum Information, University of Science and Technology of China,
Chinese Academy of Sciences, Hefei, 230026, P. R. China*

⁵*Department of Chemistry and Biochemistry, University of Maryland, College Park, Maryland 20742, USA*

⁶*Materials Sciences Division, Lawrence Berkeley National Laboratory,
1 Cyclotron Road, Berkeley, California 94720, USA*

(Dated: November 1, 2021)

Great progresses have been made in exploring exciting physics of low dimensional materials in last few decades. Important examples include the discovering and synthesizing of fullerenes (zero-dimensional, 0D) [1], carbon nanotubes (1D) [2] and graphene (2D) [3]. A fundamental question is whether we can create materials with dimensions higher than that of conventional 3D crystals, for example, a 4D crystal that has periodic structures in both space and time. Here we propose a space-time crystal of trapped ions and a method to realize it experimentally by confining ions in a ring-shaped trapping potential with a static magnetic field. The ions spontaneously form a spatial ring crystal due to Coulomb repulsion. This ion crystal can rotate persistently at the lowest quantum energy state in magnetic fields with fractional fluxes. The persistent rotation of trapped ions produces the temporal order, leading to the formation of a space-time crystal. We show that these space-time crystals are robust for direct experimental observation. The proposed space-time crystals of trapped ions provide a new dimension for exploring many-body physics and emerging properties of matter.

Symmetry breaking plays profound roles in many-body physics and particle physics [4]. The spontaneous breaking of continuous spatial translation symmetry to discrete spatial translation symmetry leads to the formation of various crystals in our everyday life. Similarly, the spontaneously breaking of time translational symmetry can lead to the formation of a time crystal [5, 6]. Intuitively, if a spatially ordered system rotates persistently in the lowest energy state, the system will reproduce itself periodically in time, forming a time crystal in analog of an ordinary crystal. Such a system looks like a perpetual motion machine and may seem implausible in the first glance. On the other hand, it has been known that a superconductor [7, 8] or even a normal metal ring [9–11] can support persistent currents in its quantum ground state under right conditions. However, the rotating Cooper pairs or electrons in a metal are homogenous in space. Thus no spatial order is mapped into temporal order and it is not a time crystal [5]. While it has been proved mathematically that time crystals can exist in principle [5, 6], it was not clear how to realize and observe time crystals experimentally.

In this paper, we propose a method to create a space-time crystal (Fig. 1a), which is also a time crystal, with cold ions in a cylindrically symmetric trapping potential. Different from electrons in conventional materials, ions trapped in vacuum have strong Coulomb repulsion between each other and have internal atomic states. The

strong Coulomb repulsion between ions enables the spontaneous breaking of the spatial translation symmetry, resulting in the formation of a spatial order that can be mapped into temporal order. The internal atomic states of ions can be utilized to cool the ions to the ground state as well as observing their persistent rotation directly by state-dependent fluorescence.

Trapped ion Coulomb crystals have provided unique opportunities for studying many-body phase transitions [12, 13] and quantum information science [14, 15]. The two most common types of ion traps are the Penning trap [16] and the Paul trap [15]. The magnetron motion of an ion in the Penning trap is an orbit around the top of a potential hill that is not suitable for studying the behavior of the ion in its rotational ground state. Here we propose to use a combination of a ring-shaped trapping potential from a variation of the Paul trap, and a weak static magnetic field. The ring-shaped trapping potential can be created by a quadrupole storage ring trap [17, 18], a linear rf multipole trap [19, 20] or other methods. As an example, we consider N identical ions of mass M and charge q in a ring trap and a uniform magnetic field B (Fig. 1b). The magnetic field is parallel to the axis of the trap. It is very weak so that it does not affect trapping. The equilibrium diameter of the ion ring is d . Figure 1c shows examples of the trapping potentials for a ${}^9\text{Be}^+$ ion in the radial plane of a quadrupole ring trap and a linear octupole trap, whose details are discussed in the

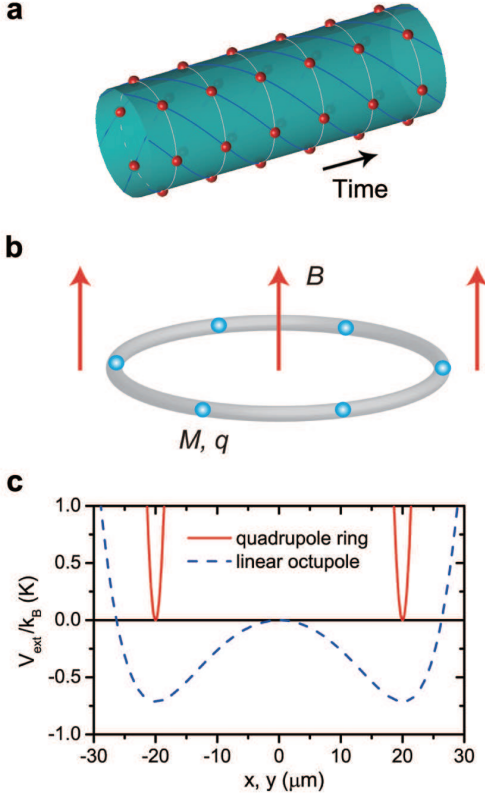


FIG. 1. **Schematic of creating a space-time crystal.** **a**, A possible structure of a space-time crystal. It has periodic structures in both space and time. The particles rotate in one direction even at the lowest energy state. **b**, Ultracold ions confined in a ring-shaped trapping potential in a weak magnetic field. The mass and charge of each ion are M and q , respectively. The diameter of the ion ring is d , and the magnetic field is B . **c**, The pseudo-potentials (V_{ext}) for a ${}^9\text{Be}^+$ ion in a quadrupole ring trap (solid curve) and a linear octupole trap (dashed curve) along the x or y axis. See Appendix for details.

Appendix section.

When the average kinetic energy of ions ($k_B T/2$, where k_B is the Boltzmann constant and T is the temperature) is much smaller than the typical Coulomb potential energy between ions, i.e. $T \ll Nq^2/(2\pi^2\epsilon_0 k_B d)$, the ions form a Wigner ring crystal. For ions in a ring crystal, we can expand the Coulomb potential around equilibrium positions to the second order. So the many-body Hamiltonian (see the Appendix section) becomes quadratic. We can diagonalize the quadratic Hamiltonian by introducing a set of N normal coordinates q_j and normal momenta p'_j . The normal coordinate and momentum of the collective rotation mode are $q_1 = \frac{1}{\sqrt{N}} \sum_j \theta_j$ and $p'_1 = \frac{1}{\sqrt{N}} \sum_j p_j$, respectively. The remaining $N-1$ normal coordinates correspond to relative vibration modes. Choosing the potential energy at equilibrium positions as the origin of energy, the Hamiltonian of the system

becomes [21]:

$$H = \frac{2\hbar^2}{Md^2} \left[\left(-i \frac{\partial}{\partial q_1} - \sqrt{N} \alpha \right)^2 + \sum_{j=2}^N \left(-\frac{\partial^2}{\partial q_j^2} + \eta^2 \omega_j^2 q_j^2 \right) \right], \quad (1)$$

where $\hbar = h/(2\pi)$ is the reduced Planck constant, $\alpha = q\pi d^2 B/(4\hbar)$ is the normalized magnetic flux, $\eta^2 = q^2 M d/(8\pi \hbar^2 \epsilon_0)$, and ω_j is the normalized normal mode frequency.

The eigenstate of this Hamiltonian is a product state $\psi(\vec{q}) = e^{ikq_1} \prod_{j=2}^N \varphi_j(q_j)$, where $\varphi_j(q_j)$ ($j \geq 2$) are eigenfunctions of harmonic oscillators. Resetting the ground state energy of the relative vibrations to be the origin of energy, the energy of this state is

$$E = \frac{2\hbar^2}{Md^2} \left[N \left(\frac{k}{\sqrt{N}} - \alpha \right)^2 + \sum_{j=2}^N 2n_j \eta \omega_j \right], \quad (2)$$

where $n_j = 0, 1, 2, \dots$ ($j \geq 2$) are the occupation numbers of the relative vibration modes. The wavefunction has to be symmetric with respect to the exchange of two identical bosonic ions, and has to be antisymmetric with respect to the exchange of two identical fermionic ions. If $n_j = 0$ for all $j \geq 2$, i.e. the relative vibration modes are in their ground states, the periodic boundary condition and symmetry property of the wavefunction requires $e^{ik(2\pi/\sqrt{N})} = 1$ for identical bosonic ions, and $e^{ik(2\pi/\sqrt{N})} = (-1)^{N-1}$ for identical fermionic ions. Thus for identical bosonic ions (e.g., ${}^9\text{Be}^+$ ions), we have $k = n_1 \sqrt{N}$ for all N , where $n_1 = 0, \pm 1, \pm 2, \dots$. For identical fermionic ions (e.g., ${}^{24}\text{Mg}^+$ ions), we have $k = n_1 \sqrt{N}$ if N is an odd number and $k = (n_1 + \frac{1}{2}) \sqrt{N}$ if N is an even number. This results a qualitatively different rotation behavior for fermions and bosons that can be observed experimentally.

The lowest normalized relative vibration frequency is $\omega_2 = 2.48$ when $N = 10$ and will increase as N increases [21]. $\omega_2 \approx \sqrt{0.32N \ln(0.77N)}$ for large N . $\eta = 4.0 \times 10^4$ for ${}^9\text{Be}^+$ ions in a $d = 10 \mu\text{m}$ ring trap. So it costs a lot of energy to excite the relative vibration modes. Thus we have $n_j = 0$ for all $j \geq 2$ at lowest energy states. For an ion ring of identical bosonic ions, the energy E_{n_1} and the angular frequency ω_{n_1} of the n_1 -th eigenstate of the collective rotation mode are:

$$E_{n_1} = E^* (n_1 - \alpha)^2 = \frac{2N\hbar^2}{Md^2} (n_1 - \alpha)^2, \quad (3)$$

$$\omega_{n_1} = \omega^* (n_1 - \alpha) = \frac{4\hbar}{Md^2} (n_1 - \alpha),$$

where $E^* = 2N\hbar^2/(Md^2)$ and $\omega^* = 4\hbar/(Md^2)$ are the characteristic energy and the characteristic frequency of the collective rotation, respectively. For identical fermionic ions, the results are the same as Eq. (3) if N is an odd number, and n_1 should be changed to $n_1 + \frac{1}{2}$ if N is an even number.

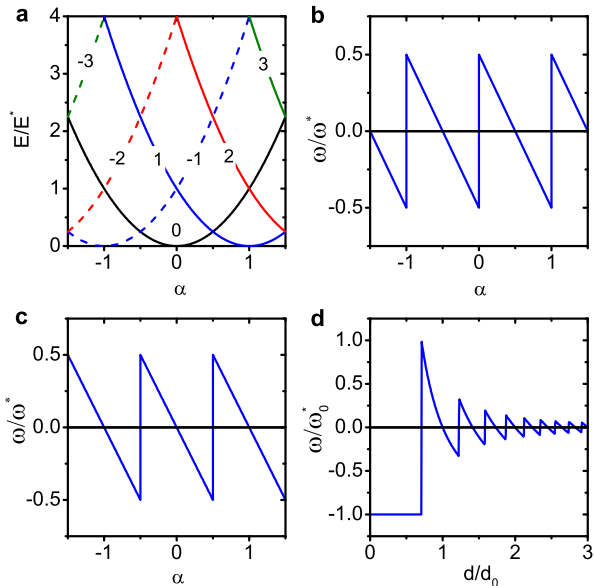


FIG. 2. **The energy levels and rotation frequencies of trapped ions.** **a**, The energy levels of identical bosonic ions as a function of the magnetic flux α . The quantum number n_1 is labeled on each curve. The angular frequency of the persistent rotation as a function α is shown in **b** for an even number of fermionic ions, and **c** for bosonic ions. **a** and **c** are also applicable to an odd number of fermionic ions. **d**, The angular frequency of the persistent rotation of a bosonic ion ring in a constant magnetic field $B_0 > 0$ as a function of its normalized diameter d/d_0 .

In classical mechanics, the angular velocity of the lowest energy state is always $\omega/\omega^* = 0$, which means that the ions do not rotate. In quantum mechanics, however, $\omega/\omega^* = 0$ is not an eigenvalue when the normalized magnetic flux α is not an integer or half of an integer. So the ions can rotate persistently even at the ground state. Since the ions are in the ground state already, there is no radiation loss due to the rotation. The rotation frequency is independent of the number of ions in the ring. The energy gap between the ground state and the first excited state is $\Delta E = N\hbar^2/(Md^2)$ when $\alpha = 1/4$. $\Delta E \rightarrow \infty$ when $N \rightarrow \infty$. Thus the persistent rotation of identical ions is a macroscopic quantum phenomenon and is robust for observation when N is large, which is important for a time crystal [5]. This is very different from the situation of a rigid body with mass NM and charge Nq in a ring, for which the maximum energy gap between the ground state and the first excited state is $\Delta E_{rigid} = 2\hbar^2/(NMd^2)$. $\Delta E_{rigid} \rightarrow 0$ when $N \rightarrow \infty$. When we consider a rigid body, we only minimize the energy of its center-of-mass (c.o.m.) motion. Here we minimize the total energy of the whole system, which depends on the internal interaction and the exchange symmetry of the system. If the relative vibration modes are not in their ground states, the symmetry requirement of the

c.o.m motion of identical particles is relaxed and the energy gap between different c.o.m. motion states becomes smaller. The result becomes the same as that of a rigid body when all particles are different from each other.

Figure 2a shows the lowest energy levels of an ion ring consisting identical bosonic ions. When the magnetic flux satisfies $-0.5 < \alpha < 0.5$, the $n_1 = 0$ state is the ground state. As α increases above 0.5, $n_1 = 1$ state becomes the ground state. Similar things happen whenever α crosses half integer values. As a result, the angular frequency of the persistent rotation of the ground state is a periodic function of the magnetic flux (Fig. 2c). Figure 2d shows the rotation frequency of a bosonic ion ring in a constant positive magnetic field B_0 as a function of its normalized diameter d/d_0 , where $d_0 = \sqrt{4\hbar/(\pi q B_0)}$. The rotation frequency in Fig. 2d is normalized by $\omega_0^* = qB_0/2M$. The ground state is $n_1 = 0$ when $d/d_0 < 1/\sqrt{2}$. The rotation frequency is independent of the ring diameter and the number of ions in the ring for this state, and oscillates and decreases to 0 when d/d_0 increases above $1/\sqrt{2}$. If we confine many ions in a harmonic trap to form a 3D spatial crystal, ions in the crystal will rotate with the same angular frequency ω_0^* and form a 4D space-time crystal when the outer diameter of the ion crystal is smaller than $d_0/\sqrt{2}$. If we confine ions in two concentric ring traps with diameters larger than $d_0/\sqrt{2}$, the rotation frequencies of the two rings can be different or the same, depending on the interaction between ions in different rings. When the ratio of the rotation frequencies of the two rings is an irrational number, the ions have an order in time but cannot reproduce their positions simultaneously in a finite period. Thus we have a time quasicrystal, in analog of a conventional spatial quasicrystal [22].

The persistent rotation of trapped ions can be detected by measuring the current generated by the ions, or inferred by probing the energy levels of the ion ring. More importantly, we can observe the persistent rotation directly by measuring the ion positions twice when N is large. For example, if we have an ion ring consisting N identical ${}^9\text{Be}^+$ ions, we can first use a pulse of two co-propagating laser beams to change the hyperfine state of one (or a small fraction) of the ions by stimulated Raman transition and use this ion as a mark (qubit memory coherence time greater than 10 s has been demonstrated with ${}^9\text{Be}^+$ ions [23]). Both laser beams are parallel to the axis of the ion ring and have waists of w_0 . We assume that w_0 is larger than the separation between neighboring ions and the pulse is very weak so that on average less than one ion is marked. This two-photon process localized the position of the mark ion with an uncertainty of about $\Delta x \sim w_0/\sqrt{2}$. The recoil momentum of the ion due to a stimulated Raman transition is $\vec{p}_1 - \vec{p}_2$, where \vec{p}_1 and \vec{p}_2 are the momenta of photons in the two laser beams. The amplitude of the transverse momentum of each photon in a Gaussian beam with waist of w_0 is about \hbar/w_0 . Thus the momentum of the ion ring is changed by

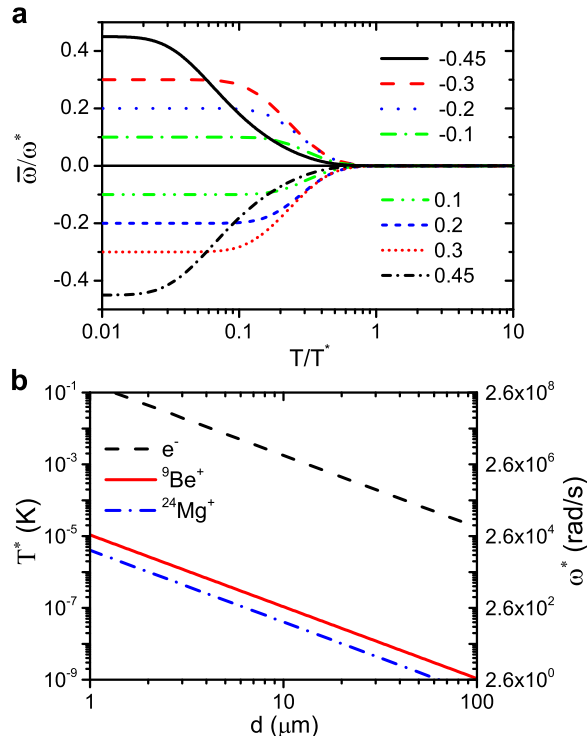


FIG. 3. **The temperature dependence of the persistent rotation of trapped ions.** **a**, The average angular frequency of the persistent rotation of identical bosonic ions as a function of the temperature. From top down, the magnetic flux increases from -0.45 to 0.45. **b**, The characteristic temperature (left axis) and the characteristic frequency (right axis) of the persistent rotation of an ion (or electron) ring consisting 100 identical ions (or electrons) as a function of the diameter. From top down, the trapped particles are electrons, $^9\text{Be}^+$ ions, and $^{24}\text{Mg}^+$ ions.

about $\Delta p \approx \sqrt{2}\hbar/w_0$. Δp should be smaller than the absolute value of the initial momentum of the ion ring, which is $N\hbar/(2d)$ when $\alpha = 1/4$. Thus the waists of lasers need to satisfy $2\sqrt{2}d/N < w_0 < \sqrt{2}d$ in order to localize the position of an ion without significantly alter the initial momentum of the ion ring. This condition can be fulfilled when N is large. Then we can use a global probe laser which is only scattered by the mark ion [24] (state-dependent fluorescence) to measure its angular displacement ($\Delta\theta_{mk}$) after a time separation Δt . The displacement of the mark is about $\Delta\theta_{mk} \approx \omega^*(n_1 - \alpha)\Delta t$ when N is large. The mark ion repeats its position when $\Delta t \approx 2\pi l / [\omega^*(n_1 - \alpha)]$, where l is an integer. After the measurement, we can cool the ions back to the ground state and repeat the experiment again.

To study the effects of finite temperatures on persistent rotation, we assume the trapped ions are at thermal equilibrium with temperature T . Then the average an-

gular frequency of the ions is

$$\bar{\omega} = \sum_{n_1=-\infty}^{\infty} \frac{\omega_{n_1}}{Z} e^{-E_{n_1}/k_B T}, \quad (4)$$

where the partition function is $Z = \sum_{n_1} e^{-E_{n_1}/k_B T}$. It is convenient to define $T^* \equiv E^*/k_B = N\hbar\omega^*/2k_B$ as the characteristic temperature for the ring of ions. T^* increases when N increases.

Figure 3a shows the average rotation frequency of an ion ring consisting identical bosonic ions as a function of the temperature. At very low temperatures ($T \ll T^*$), the average rotation frequency is independent of the temperature. As the temperature increases, the probability of the ion ring occupying excited states increases. These states have positive and negative velocities alternately, which cancel each other. As a result, the amplitude of the average rotation frequency drops to zero at high temperatures ($T > T^*$). So T^* can be considered as the phase transition temperature of the space-time crystal. T^* and ω^* as a function of the diameter of an ion ring (or an electron ring) are displayed in Fig. 3b. For a $d = 100 \mu\text{m}$ ion ring consisting 100 $^9\text{Be}^+$ ions, $T^* = 1.1$ nK and $\omega^* = 2.8$ rad/s. T^* is larger for smaller ion rings.

In order to experimentally realize such a space-time crystal with trapped ions, we need to confine ions tightly to have a small d , and cool the ions to a very low temperature. Recently, cylindrical ion traps with inner radius as small as $1 \mu\text{m}$ have been fabricated [25]. Simulations suggested that it is also possible to confine charged particles with a nanoscale rf trap [26]. The challenge is that ions must be cooled to below $1 \mu\text{K}$ for a microscale trap (Fig. 3b). We propose to first add a pinning potential to confine ions with MHz trapping frequencies in the circumference direction. A combination of Doppler cooling and resolved-sideband cooling can be used to cool the ions to the ground state of the MHz trap [15, 27]. The system is in the ground state of the ring-shaped trapping potential after ramping down the pinning potential adiabatically. For $T^* = 1.1$ nK, the ramping down time should be longer than 7 ms. Another way to achieve an ultralow temperature of ions is to put the ions near a Bose-Einstein condensate of neutral atoms [28], which has been cooled to below 0.5 nK by adiabatic decompression [29].

In conclusion, we propose a method to create and observe a space-time crystal experimentally with trapped ions. We also discuss about how to create a time quasicrystal. The space-time crystals of trapped ions provide a new dimension for studying many-body physics and may have potential applications in quantum information for simulating other novel states of matter [30].

This work was supported by NSF Nanoscale Science and Engineering Center (CMMI-0751621). Z.X.G and L.M.D were supported by NBRPC (973 Pro-

gram) 2011CBA00300 (2011CBA00302), the IARPA MUSIQ program, the ARO and the AFOSR MURI program. Z.Q.Y. was supported by NBRPC (973 Program) 2011CBA00300 (2011CBA00302), NNSFC 61073174, 61033001, 61061130540, 11105136, and Postdoc Research Funding of China Grant 20110490829. H.T.Q. was supported by NSF Grant No. DMR-0906601.

APPENDIX

Quadrupole ring trap. A rf quadrupole ring trap can be formed by many segments of quadrupole electrodes [17] or four ring electrodes [18]. The harmonic pseudo-potential for a single ion is $V_{ext}(r, z) = \frac{1}{2}M\omega_r^2(r - r_{min})^2 + \frac{1}{2}M\omega_z^2z^2$, where $r = \sqrt{x^2 + y^2}$ is the radial position of the ion, r_{min} is the radius of the ring trap, ω_r and ω_z are trapping frequencies in the radial and axial (z) directions, respectively. If the inner radius of the trap (r_0 , which is half of the separation between opposite electrodes [17]) is much smaller than r_{min} , the trapping frequencies are approximately $\omega_r = \omega_z = qV_{rf}/(\sqrt{2}M\Omega r_0^2)$. Here V_{rf} is the amplitude of the rf voltage applied to adjacent electrodes, $\Omega/2\pi$ is frequency of the rf voltage. In Fig. 1c, $\omega_r = 2\pi \times 5$ MHz and $r_{min} = 20 \mu\text{m}$ for the quadrupole ring trap.

Linear rf multiple trap. The pseudo-potential for a single ion in a linear rf multipole trap is cylindrically symmetric [19, 20]:

$$V_{ext}(r, z) = \frac{k^2 q^2 V_{rf}^2}{16M\Omega^2 r_0^2} \left(\frac{r}{r_0}\right)^{2k-2} + \frac{\beta q V_{dc}}{z_0^2} \left(z^2 - \frac{r^2}{2}\right),$$

where $2k$ is the number of poles of the trap, β is the geometrical factor of the trap, V_{dc} is the static voltage applied to the outside sets of segmented electrodes, and $2z_0$ is the length of the center part of the segmented trap. The trapping frequency in the axial direction is $\omega_z = \sqrt{2\beta q V_{dc}/(Mz_0^2)}$. The trapping potential has its minimum value in the radial direction at

$$r_{min} = r_0 \left(\frac{2M\Omega\omega_z r_0^2}{qV_{rf}k\sqrt{k-1}} \right)^{1/(k-2)}.$$

The trapping frequency in the radial direction is $\omega_r = \sqrt{k-2}\omega_z$ near r_{min} . Fig. 1c shows an example of the effective trapping potential for a ${}^9\text{Be}^+$ ion in the radial plane of an octupole trap ($2k = 8$). The parameters used for the calculation of Fig. 1c are $r_0 = 200 \mu\text{m}$, $V_{rf} = 200$ V, $\omega_z/2\pi = 0.5$ MHz, and $\Omega/2\pi = 94$ MHz.

Many-body Hamiltonian. As we are interested in the rotation of ions in a ring at very low temperatures, our Hamiltonian only involves the angular coordinate θ_j ($j = 1, \dots, N$) of trapped ions:

$$H = \sum_{j=1}^N \frac{(p_j - qA_\theta)^2}{2M} + \sum_{j<l} \frac{q^2}{4\pi\epsilon_0 d |\sin(\frac{\theta_j - \theta_l}{2})|},$$

where $p_j = -i\frac{2\hbar}{d}\frac{\partial}{\partial\theta_j}$ is the canonical momentum operator, $A_\theta = Bd/4 = \phi/(\pi d)$ is the vector potential, and ϵ_0 is the electric constant of vacuum. $\phi = \pi d^2 B/4$ is the magnetic flux inside the ion ring.

* Corresponding author: xiang@berkeley.edu

- [1] H. W. Kroto, J. R. Heath, S. C. O'Brien, R. F. Curl, and R. E. Smalley, *Nature* **318**, 162 (1985).
- [2] S. Iijima, *Nature* **354**, 56 (1991).
- [3] K. S. Novoselov, A. K. Geim, S. V. Morozov, D. Jiang, Y. Zhang, S. V. Dubonos, I. V. Grigorieva, and A. A. Firsov, *Science* **306**, 666 (2004).
- [4] F. Strocchi, *Symmetry breaking*, 2nd ed. (Springer, Heidelberg, 2008).
- [5] F. Wilczek, "Quantum time crystals," (2012), arXiv:1202.2539v1.
- [6] A. Shapere and F. Wilczek, "Classical time crystals," (2012), arXiv:1202.2537v1.
- [7] N. Byers and C. N. Yang, *Phys. Rev. Lett.* **7**, 46 (1961).
- [8] J.-X. Zhu and H. T. Quan, *Phys. Rev. B* **81**, 054521 (2010).
- [9] M. Büttiker, Y. Imry, and R. Landauer, *Phys. Lett.* **96A**, 365 (1983).
- [10] L. P. Lévy, G. Dolan, J. Dunsmuir, and H. Bouchiat, *Phys. Rev. Lett.* **64**, 2074 (1990).
- [11] A. C. Bleszynski-Jayich, W. E. Shanks, B. Peaudecerf, E. Ginossar, F. von Oppen, L. Glazman, and J. G. E. Harris, *Science* **326**, 272 (2009).
- [12] Z.-X. Gong, G.-D. Lin, and L.-M. Duan, *Phys. Rev. Lett.* **105**, 265703 (2010).
- [13] K. Kim, M.-S. Chang, S. Korenblit, R. Islam, E. E. Edwards, J. K. Freericks, G.-D. Lin, L.-M. Duan, and C. Monroe, *Nature* **465**, 590 (2010).
- [14] J. I. Cirac and P. Zoller, *Phys. Rev. Lett.* **74**, 4091 (1995).
- [15] D. Leibfried, R. Blatt, C. Monroe, and D. Wineland, *Rev. Mod. Phys.* **75**, 281 (2003).
- [16] L. S. Brown and G. Gabrielse, *Rev. Mod. Phys.* **58**, 233 (1986).
- [17] T. Schätz, U. Schramm, and D. Habs, *Nature* **412**, 717 (2001).
- [18] M. J. Madsen and C. H. Gorman, *Phys. Rev. A* **82**, 043423 (2010).
- [19] K. Okada, K. Yasuda, T. Takayanagi, M. Wada, H. A. Schuessler, and S. Ohtani, *Phys. Rev. A* **75**, 033409 (2007).
- [20] C. Champenois, M. Marcianti, J. Pedregosa-Gutierrez, M. Houssin, M. Knoop, and M. Kajita, *Phys. Rev. A* **81**, 043410 (2010).
- [21] G. Burmeister and K. Maschke, *Phys. Rev. B* **65**, 155333 (2002).
- [22] D. Levine and P. J. Steinhardt, *Phys. Rev. B* **34**, 596 (1986).
- [23] C. Langer, R. Ozeri, J. D. Jost, J. Chiaverini, B. DeMarco, A. Ben-Kish, R. B. Blakestad, J. Britton, D. B. Hume, W. M. Itano, D. Leibfried, R. Reichle, T. Rosenband, T. Schaetz, P. O. Schmidt, and D. J. Wineland, *Phys. Rev. Lett.* **95**, 060502 (2005).
- [24] A. H. Myerson, D. J. Szwer, S. C. Webster, D. T. C. Allcock, M. J. Curtis, G. Imreh, J. A. Sherman, D. N. Stacey, A. M. Steane, and D. M. Lucas, *Phys. Rev. Lett.*

- 100**, 200502 (2008).
- [25] D. Cruz, J. P. Chang, M. Fico, A. J. Guymon, D. E. Austin, and M. G. Blain, *Rev. Sci. Instrum.* **78**, 015107 (2007).
- [26] D. Segal and M. Shapiro, *Nano Lett.* **6**, 1622 (2006).
- [27] C. Monroe, D. M. Meekhof, B. E. King, S. R. Jefferts, W. M. Itano, D. J. Wineland, and P. Gould, *Phys. Rev. Lett.* **75**, 4011 (1995).
- [28] C. Zipkes, S. Palzer, C. Sias, and M. Köhl, *Nature* **464**, 388 (2010).
- [29] A. E. Leanhardt, T. A. Pasquini, M. Saba, A. Schirotzek, Y. Shin, D. Kielpinski, D. E. Pritchard, and W. Ketterle, *Science* **301**, 1513 (2003).
- [30] R. Blatt and C. F. Roos, *Nature Phys.* **8**, 277 (2012).